Heliyon 10 (2024) e36410

Contents lists available at ScienceDirect

Heliyon

journal homepage: www.cell.com/heliyon

Review article

Influenza viruses and SARS-CoV-2 diagnosis via sensitive testing methods in clinical application

Le Zhang [a,b,1], Chunwen Li [c,1], ShaSha Shao [a], Zhaowei Zhang [d,*], Di Chen [a,**]

[a] Department of Critical Care Medicine, Tongji Hospital, Tongji Medical College, Huazhong University of Science and Technology, Wuhan 430030, China
[b] School of Ecology and Environment, Tibet University, Lhasa 850000, China
[c] Department of Emergency Medicine, The Second Affiliated Hospital of Chongqing Medical University, Chongqing 400010, China
[d] State Key Laboratory of New Textile Materials and Advanced Processing Technologies, School of Bioengineering and Health, Wuhan Textile University, Wuhan, 430200, China

ARTICLE INFO

Keywords:
Point of care test
Influenza viruses
SARS-CoV-2
Rapid
Sensitivity

ABSTRACT

The identification of influenza viruses and SARS-CoV-2 has garnered increasing attention due of their longstanding global menace to human life and health. The point-of-care test is a potential approach for identifying influenza viruses and SARS-CoV-2 in clinical settings, leading to timely discovery, documentation, and treatment. The primary difficulties encountered with conventional detection techniques for influenza viruses and SARS-CoV-2 are the limited or inadequate ability to identify the presence of the viruses, the lack of speed, precision, accuracy, sensitivity, and specificity, often resulting in a failure to promptly notify disease control authorities. Recently, point-of-care test methods, along with nucleic acid amplification, optics, electrochemistry, lateral/vertical flow, and minimization, have been demonstrated the characteristics of reliability, sensitivity, specificity, stability, and portability. A point-of-care test offers promising findings in the early detection of influenza viruses and SARS-CoV-2 in both scientific research and practical use. In this review, we will go over the principles, advantages, limitations, and real-world applications of point-of-care diagnostics. The significance of constraints of detection, throughput, sensitivity, and specificity in the analysis of clinical samples in settings with restricted resources is underscored. This discussion concludes with their prospects and challenges.

1. Introduction

Influenza virus (IVs) and SARS-CoV-2 are the most common infectious diseases (A. [1]), causing fever, coughing, pneumonia, asthma, and cardiovascular disease ([2], T. M. [3]). The prevention and control of IVs and SARS-CoV-2 are challenging due to their rapid and intricate mode of transmission, such as by respiratory droplets. Influenza viruses (IVs) and the SARS-CoV-2 virus have contributed to the occurrence of flu seasons, infecting approximately 15 % of the global population. This has resulted in millions of individuals experiencing severe illnesses and a death toll of 0.6 million within a single year. Notable instances of pandemics include the influenza outbreaks in Spain (1918–1920), Asia (1957), Hong Kong (1968), Russia (1977), and swine flu (2009). IVs administration of

* Corresponding author.
** Corresponding author.
E-mail addresses: zwzhang@whu.edu.cn (Z. Zhang), 2012tj0562@hust.edu.cn (D. Chen).
[1] These authors contributed equally to this work.

https://doi.org/10.1016/j.heliyon.2024.e36410
Received 13 March 2024; Received in revised form 2 July 2024; Accepted 14 August 2024
Available online 21 August 2024

substances A, B, C, or D has an impact on avian species that inhabit aquatic environments ([4], Jolianne M. [5,6]), cattle [7], pigs ([8,9], Karl A. [10], Gustavo [11,12]), mammals [13], and humans [14,15]. Type IV, which belongs to the orthomyxoviridae family, has been responsible for four international pandemics that have killed billions of people. Influenza viruses of type A (IVAs) have the ability to infect both humans and animals, whereas type B (IVB) and type C (IVC) influenza viruses are more inclined to infect humans ([16], Sankar [17], Pinjia [18,19]). The typical methods used for virus detection include serological detection, blood analysis, viral antigen detection, viral nucleic acid detection, viral isolation and culture identification, enzyme-linked immunosorbent test, and chest X-ray inspection [20]. Early virus detection is almost essential to timely and sensitively track the epidemiology of the epidemic and find the patient via powerful digital tools. For example, in the virus envelope, the glycoproteins hemagglutinin, neuraminidase, and nucleoprotein are wrapped around a central core screen of the special antibody in lab-on-a-chip or lateral flow methods (S. [21]) (see Table 1).

Point-of-care testing (POCT) approaches are favored for the detection of human IVs and SARS-CoV-2 due to their rapidity, non-invasive nature, portability, simplicity for untrained staff, minimal number of steps, and suitability for resource-limited settings [22]. POCT devices integrate electronic medical records to rapidly record and disseminate test data while evaluating IVs and SARS-CoV-2. Introducing portable readouts or mobile equipment enables immediate diagnosis and treatment, hence decreasing the time it takes to complete a task and conserving additional medical resources [23] Principally, the POCT includes three steps: target recognition, signal transition, and result record. First, an antibody, aptamer, epitope protein, DNA, or RNA recognizes the target of interest. Second, the recognition signal will be amplified and/or transferred to another signal type for facilitated recording. Third, the signal is calculated using a portable reader or a smartphone app depending on the target concentration. The turn-around time will be from several min utes via a test strip or several hours in PCR, dramatically shorter than previously instrument-based clinical detection [24].

POCT detection methods have been widely employed in practice due to their flexibility, resulting in the creative utilization of several detection instruments. POCT devices encompass a range of technologies, including traditional procedures, sensors, and new techniques. Traditional techniques such as nucleic acid amplification [25], ELISA (T. [26]). Sensors including optical, electricity, lateral flow and vertical flow (Mengdan Lu et al., 2022), microfluidics [27]. Point-of-care testing (POCT) devices enhance the efficiency and speed of collecting, processing, and transmitting test findings. The integration of cellphones in point-of-care testing (POCT) holds promise for the intelligent detection of IVs. Smartphones have the capability to directly capture testing signals using their cameras or transmit the testing signal to cloud data for the purpose of sharing. Smartphones offer convenient access to optical, microscopic, and electrochemical testing methods. The progress of intelligent point-of-care testing (POCT) significantly enhances the ability to self-diagnose and self-monitor IVs treatments and SARS-CoV-2 infections (M. [28]). These point-of-care testing (POCT) devices have been widely recognized as developing commercial items.

Several commendable evaluations on Point-of-Care Testing (POCT) in clinical applications have concentrated on fundamental details, such as principles and testing formats. Our focus is on Point-of-Care Testing (POCT) for IVs in humans and the clinical applications of testing for the SARS-CoV-2 virus. In terms of clinical application, we explored the utilization of Point-of-Care Testing (POCT) in IVs and its relevance to detecting SARS-CoV-2 in actual samples. The conventional point-of-care testing (POCT) techniques for IVs and SARS-CoV-2 are examined and contrasted with laboratory-based diagnostic approaches, such as optics, electrochemistry, test strip, and enzyme-linked immunosorbent assay (ELISA). An assessment is conducted on the growing point-of-care testing (POCT)

Table 1
The pros and cons of POCT devices.

Methods		Pros	Cons
Conventional methods	PCR testing methods	high sensitivity/High specificity and accuracy/Safe and pollution-free/good reproducibility/High throughput detection capability	Easy contamination/cumbersome operation/presence of non-specific amplification/low concentration sample detection accuracy and sensitivity are insufficient
	Isothermal amplification testing methods	Easy to operate/High specificity/suitable for rapid field detection/simple equipment	Sensitivity may be limited/specific primers and enzymes are required/experimental conditions are more demanding/non-specific amplification may occur
Sensor methods	Optical testing methods	Fast results/portability/easy operation/high accuracy	High cost/requires regular maintenance and calibration/may be affected by environmental factors
	Electrical testing methods	Fast/portable/easy to operate/real-time feedback	Higher costs/training needs for operators/quality control and standardization/dependence on electricity
	Lateral flow and vertical flow testing methods	Fast detection/low cost/easy operation/Wide applicability/Good chromatographic separation/suitable for complex samples/automation potential	Precision limitation/Sensitivity limitation/qualitative rather than quantitative
	Minimized testing methods	Portability and mobility/Rapid diagnostics/simplified operational processes/Reduced sample handling and shipping costs	High cost/establish quality control and standardization/rely on electricity and stable operating environment
Other methods	Smartphone-based testing methods	Portability and mobility/Quick diagnosis/User friendliness/real-time feedback/cost reduction/high technology integration	Equipment compatibility issues/data security and privacy protection/accuracy of test results/power supply/technical updates and upgrades/Regulation and standards required
	Pressure-based testing methods	Quick diagnosis/Simplified operation/portability/real-time feedback	Technology maturity/low accuracy and accuracy/sample preparation requirements/equipment maintenance and calibration/application field limitations

techniques, such as microfluidics and cellphones. Furthermore, the difficulties associated with commercialized point-of-care testing (POCT) products are addressed. This approach has the potential to provide valuable insights for fundamental research that can be applied in practical settings.

2. Conventional testing methods

2.1. PCR testing methods

PCR procedures recognized by authorities are utilized for the detection of numerous infectious agents (M. [29,30]). The cobas® Influenza A/B assay (Roche Diagnostics, USA) has been approved by the Food and Drug Administration. It is utilized to qualitatively

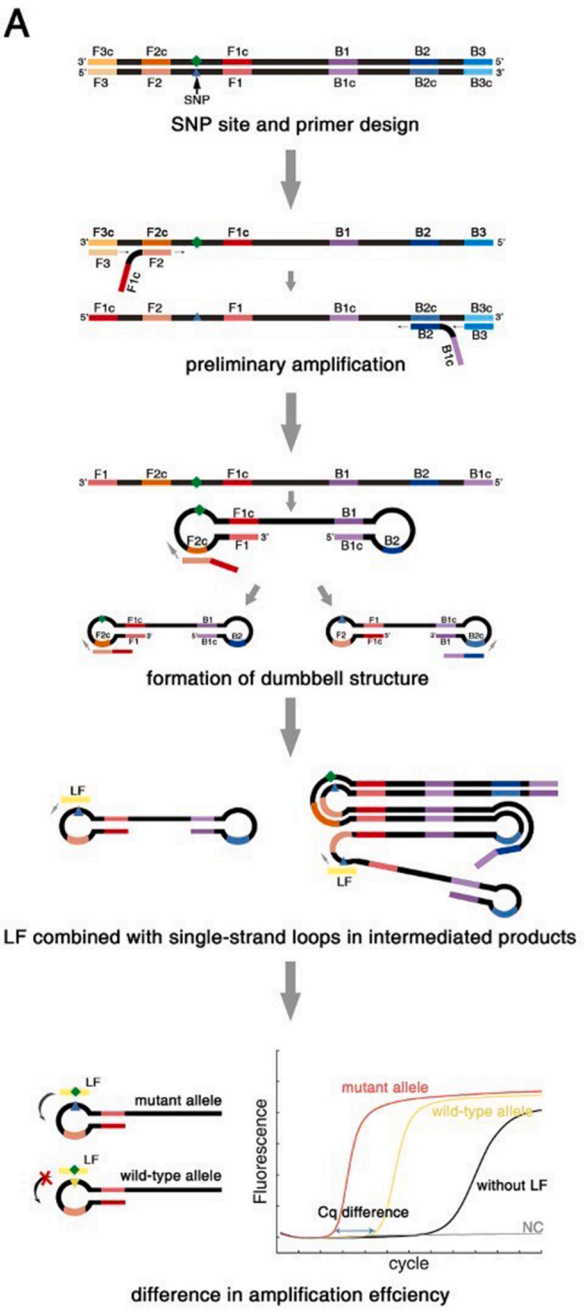

Fig. 1.

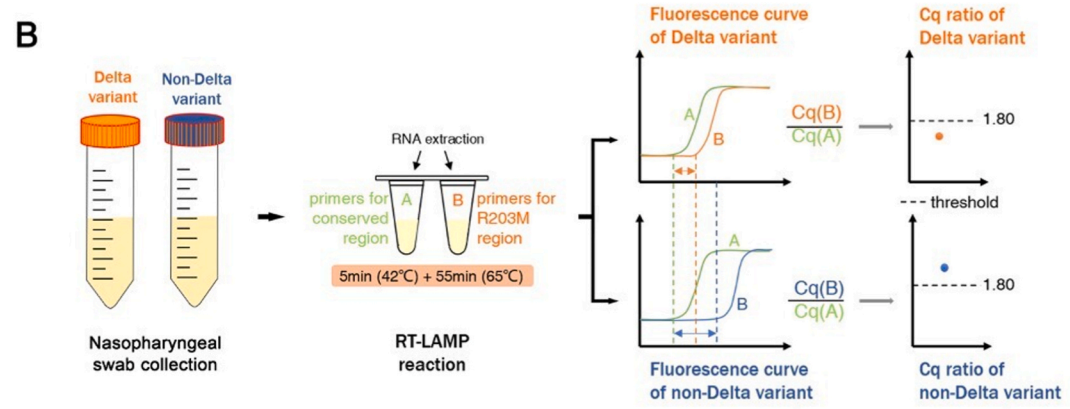

Fig. 1. (*continued*).

screen for Influenza A/B in 300 fresh and frozen nasopharyngeal swab specimens within a 20-min timeframe (L. [31]). Another study investigated the above assay and Alere™ i Influenza A & B assay (Alere group, USA) using 87 samples from adults [32]. In the study conducted by Ref. [33], the detection of IVA H3N2 involved trapping the amplicons on silica beads using a size-selective capture chamber (8 nL) on a microchip. This was followed by a fluorescence readout using a tiny photodiode. The utilization of a 5 μL sample resulted in a low limit of detection (LOD) for nucleic acids. It was compatible with the commercial PCR counter, allowing for a decrease in sample quantities from 25 to 5 μL.

PCR influenza virus primer design is a very important premise in PCR POCT. The efficiency and specificity of PCR reaction depend on the precise sequence complementation of primer and template. According to the FLU sequence database (http://www.ncbi.nlm.nih.gov/genomes/on FLU/FLU. HTML) sequence information design qRT - PCR primers and probe the Beacon Designer (version7.6) software (Premier Biosoft) was used to compare each available virus sequence in the database, and primers and probes were designed to specifically target highly conserved regions of these sequences [34]. The researchers investigated several IVC sequences, including 141 hemagglutinin-esterase, 106 matrix, and 97 nucleoprotein sequences, using specifically designed primers and probes. They found that the limit of detection (LOD) was between 10 and 100 RNA copies per reaction, as reported by Ref. [35]. The Food and Drug Administration approved fast PCR kits (Cobas & Roche) for the detection and differentiation of Influenza Virus A (IVA) and Influenza Virus B (IVB) (M. J. [36]). Testing time was reduced from 60 min by the real-time PCR assay (Simplexa Flu A/B & RSV Direct) to 20 min. A satisfied agreement of 99.5 % was recorded between these two PCR kits, using 197 clinical swab samples, including 123 specimens (nasopharyngeal swabs), 141 throat swabs, and 22 nasal swabs.The Cobas Liat platform required less than 5 min, whereas the entire process took 20 min.

For multiple IVs detection, an ePlex Respiratory Pathogen Panel (GenMark Diagnostics) targeted nineteen viruses (N. E. [37]). A total of 2908 nasopharyngeal swab specimens were used to validate the panel, using the bioMérieux/BioFire FilmArray Respiratory Panel as a reference. The overall agreement between the two methods was 95 %. The agreement for positive percentages ranged from 85.1 % to 95.1 %, whereas for negative percentages it ranged from 99.5 % to 99.8 %. It exhibits a reproducibility rate of 100 %. A charge-transfer complex with high efficiency for capturing large amounts of RNA was established and compatible with high-speed qRT-PCR kit. The entire process from extraction to identification can be completed within 1 h. Four substances (influenza virus, SARS-CoV-2 and its δ and plasmid variants) were detected in 260 clinical samples with a sensitivity of 99.4 % and a specificity of 98.9 % [38].

A high-capacity fluorescence digital PCR approach was proposed for the detection of IVs and SARS-CoV-2, which can attain a high level of sensitivity. When the concentration of IV is below 10 copies, the signal-to-noise ratio closely resembles that of a single molecule in each reaction, and there is no occurrence of cross-reaction. Clinical practical sample detection can achieve 100 % accuracy (Z. J. [39]). The Luminex ARIES® Flu A/B & RSV can realize the automated real-time PCR assay for IVA, IVB, and RSV. Compared to the Cepheid Xpert® Flu/RSV XC assay, 143 nasopharyngeal specimens were tested, resulting in an agreement of 96.6%–100 % (P. [40]). The advantage of Xpert® Flu/RSV XC assay was reduced turn-around-time from 120 to 60 min.

2.2. Isothermal amplification testing methods

The isothermal amplification (P. [41]), like reverse transcriptase loop-mediated isothermal amplification (RT-LAMP) (M. [42], S. Y. [43]), piecewise isothermal nucleic acid test (S. [44]), or supercritical angle fluorescence array (T. L. [45]) can be applied solely or integrated with microfludics (W. I. [46]). SARS-CoV-2, IVA, and IVB can be extracted, amplified, and detected via colorimetric RT-LAMP based on a capillary flow on a paper (D. [47]). The RT-LAMP assay for SARS-CoV-2 was completely concordant with standard RT-qPCR. The test differentiates between delta variants and non-delta variants, and the area under the curve was 1.00 [48] (Fig. 1). The microdevice integrated RT-LAMP to purify RNA via microbead and real-time monitor RT-LAMP with a miniaturized optical detector (J. H. [49]). To purify RNA or lysates of IVA RNA, they set several reservoirs, including the washing buffer (70 % EtOH), elution buffer (RNase-free water), a RT-LAMP cocktail, and two chambers. RT-LAMP primer sets specifically targeted IVAs

(H1N1, H3N2, H5N1) as RNA templates. Subsequently, IVA RNA was isolated by employing microbeads and centrifugation, and then subjected to gene amplification via RT-LAMP using a cocktail. IVA H1N1 was discovered within a time frame of 47 min, with a sensitivity 10 times greater than that of RT-PCR, at a concentration of ten copies.

Although the isothermal amplification method has the advantage of being fast and sensitive in virus detection. However, the generation of false positives and the limited multiplicity are the main bottlenecks that must be solved. A multiple A rgonaute (Ago) n nucleic acid detection system (MULAN) was established to detect SARS-CoV-2 and influenza viruses simultaneously. Through the validation of clinical samples, it was confirmed that the method was 100 % consistent with the PCR results (X. [50]). This shows that this isothermal amplification system has great development potential in the real-time diagnosis of viruses.

2.2.1. CRISPR/Cas testing methods

In order to overcome the limitations of amplification and expensive instruments, CRISPR diagnosis, which relies on enzyme activity, has become a new way to detect viruses. CRISPR has the advantage of being fast, robust and sensitive. CRISPR-Cas3 collateral single-strand DNA cleavage provides a rapid and accurate immediate detection of IVA in clinical samples. This method has the potential for rapid (within 40 min), low-cost, instrument-free detection of IVA [51]. The CRISPR/Cas13a system and hybridization chain Reaction (HCR) were used for colorimetric biosensor assay of H1N1 influenza virus. The target RNA of H1N1 activates the trans-cutting activity of Cas13a, cuts the -UUU - sequence of the probe, and then initiates HCR, produces a large amount of G-rich DNA, and catalyzes the colorimetric reaction. The sensitivity of the method, which has a detection limit of 0.152 pM, makes it a promising method for rapid influenza diagnosis [52]. For cross-free simultaneous detection, the diagnostic test with CRISPR coupled with RT-RPA and RT-LAMP can detect IAV and IBV in 75–85 min. The detected IAV and IBV titers are as low as 1×100. The results were also validated using a transverse flow bar assay that does not require additional analytical equipment [53].

When the traditional nucleic acid technology is combined with detection technology, visual detection of virus can be realized. Not only improve the detection time, but also improve the accuracy of clinical samples.

3. Sensor testing methods

3.1. Optical testing methods

3.1.1. Fluorescence testing methods

The in-tube-based homogeneous POCT has been investigated for IVA detection with fluorescence. Quantum dot (QD) aptamer beacons with light guides can use to detect IVA (H1N1), in which the fluorescent signals were captured by a home-made setup with the camera of a smartphone [54]. A luminescent resonance energy transfer sandwich method with up-conversion nanoparticles and Au nanoparticles as donors or acceptors, respectively, was developed for the highly sensitive (LOD of 134×10^{-12} m) and rapid determination (40 min) of IVA H7N9 (M. K. [55]).

The fluorescence point-of-care test (POCT) has the capability to identify numerous IVs. The simultaneous detection of H1N1 and H5N1 was achieved by combining a fluorescent probe based on Ag nanoclusters emitting at 520 and 600 nm with target recognition in a single step (G. L. [56]). The IVA recognition induced Ag nanoclusters beacon conformational transition, finding LODs of 2 nM and 10 nM for IVA. Multiple IVAs (H1 to H16) were visually detected, assisted by peptide nucleic acid and Au nanoparticles reporter. Non-complementary viral RNA sequence induced free peptide nucleic acid-induced aggregation of Au nanoparticles, inducing color change. A LOD of 2.3 ng was recorded in cloacal samples on a simple spectrophotometer by using an absorption ratio of A640/A520 (N. [57]).

Near field optics and optical tunneling light matter can interact with QD, which makes it possible to detect chiral analytes of POCT. In a chiroimmunosensor, Ahmed et al. (S. R. [58]) developed the asymmetric plasmonic chiral nanostructures via self-assembly for extending spectral from circular dichroism with QD excited state. This chiroimmunosensor obtained lower LOD in blood for IVA (H4N6) at the picomolar level, namely, 0.0315 HAU/50 μL, and range from 100 to 0.01 HAU/50 μL.

3.1.2. SPR testing methods

SPR POCT demonstrated a high sensitive technique down to the fM The study by Meryem B. et al. [59] investigated the threshold for detecting IVA using either the colorimetric or fluorescence format. Au is the standard signal source. A colorimetric surface plasmon resonance (SPR) method was used to identify the presence of SARS-CoV-2 using gold nanoparticles. The visible alteration in the color of gold nanoparticles was a result of the deactivation of mercapto-modified antisense oligonucleotides triggered by SARS-CoV-2 RNA. The minimum detectable concentration was 0.18 ng per milliliter in nasal swabs (P. [60]). A localized SPR (LSPR) enabling fluorescent nano POCT was illustrated (K. [61]) with enhanced LSPR signal from the interaction of IVA antigens and anti-neuraminidase Ab@Au NPsQDs. LODs for IVA and H1N1 were 0.4 pg mL^{-1} in human serum. The active dynamic sensing platform of LSPR was established by modulating the external magnetic field. For clinically isolated H3N2, the LOD was 10 PFU mL^{-1}, 25 orders of magnitude higher sensitivity compared with previous LSPR, HPLC, LFA, electrochemistry [62].

The sensitivity can be enhanced by employing magnetic plasmonic gyro-nanodisks (GNDs). The GND-based FT-SPR utilizes the magnetic responsiveness of GND to generate a periodic extinction signal in the surface plasma band when subjected to an external rotating magnetic field. The attachment of an Influenza A virus (IVA) H1N1 to graphene nanodots (GNDs) increased the magnitude of the applied force and caused a shift in the frequency range. The sensitivity is enhanced by 75 pM through the modulation of the number and placement of plasma GNDs [63]. The signal enhancement can be achieved by Au NPs-induced quaternary CdSeTeS QD fluoresce. Interestingly, short peptides can regulate the distance between quantum dots and Au nanoparticles, and IVA H1N1 has a minimum

LOD of 17.02 fg mL^{-1} between 10^{-14} and 10^{-9} g mL^{-1} (F. [64]).

To improve the detection throughput, functionalized surface-glycosylated microbeads selectively captured IVs. S-chain glycosides have affinity for a variety of IVs. SPR iPOCT increased detection limits (30 times) by adding magnetic beads. The release of captured virus does not reduce primary infectivity and the recovery rate is 50 % [24] (Fig. 2).

3.1.3. SERS testing methods

SERS labels can improve the detection sensitivity, and when combined with POCT, they can enhance the quantitative ability, such as 5,5-dithiobis-(2-nitrobenzoic acid) (DTNB) and calcium ions. Fe_3O_4/DTNB@Ag/DTNB as magnetic SERS nanotags can be used to recognize and enrich IVAs without any sample pre-treatment. Wang et al. (C. W. [65]) investigated a SERS-based LFA for simultaneous detection of IVA H1N1 and adenovirus within 30 min by using dual-dye-modified Fe_3O_4/DTNB@Ag/DTNB. The sensitivity of the 2000-fold increase was superior to that of the colloidal gold approach, reaching a detection limit of 10 pfu mL-1. The addition of acetonitrile and calcium ions to silver nanoparticles was employed to increase the surface-enhanced Raman scattering (SERS) effect. This enhancement enables the highly sensitive detection of the new coronavirus [66]. The method stimulated the highly sensitive SERS signal of viruses, and successfully captured the characteristic SERS signal of SARS-CoV-2 and IVs at the concentration of 100 copies $time^{-1}$ (PFU $time^{-1}$), with good reproducibility and signal-to-noise ratio in the saliva and serum. Au nanoparticles can be used as a substrate for SERS such as influenza virus detection. An instance of this is when the DNA aptamers of SARS-CoV-2 and influenza A/H1N1 are attached to the Au nanopopcorn substrate, creating a two-mode surface-enhanced Raman scattering (SERS) adaptive sensor. The test has the ability to precisely identify and differentiate between Severe acute Respiratory SARS-CoV-2 and influenza A (H1N1) at the same time. The LOD was measured to be 0.62 HAU mL^{-1} [67].

For multi-virus detection, a lateral flow strip with 2x3 microarray based on SERS nanotags achieved 11 pathogens detection simultaneously. The method demonstrated a broad linear dynamic range and ultra-high sensitivity because of the high surface area of nitrocellulose membrane and SERS nanotags (D. [68]). A platform with SERS and machine learning was built to detect the 13 viruses. The method used SiO_2-coated Ag nanorod array substrates to improve the sensitivity. Spectral processing programs and machine learning algorithms accurately classified virus species, strains and variants (with 99 % accuracy) [69].

To reduce the testing procedure and reagent dosage, a digital microfluidic is used in the SERS platform, due to its high automatization. For example, SERS labels of 4-mercaptobenzoic acid were synthesized with Ab@magnetic beads, showing a lower LOD of 74 pg mL^{-1} in caparison with ELISA to detect H5N1 in human serum, consuming less than 1 h and a 30 μL sample [70].

The application of fluorescence technology, SPR, and SERS have greatly improved the sensitivity of virus detection. Combined with the use of the reader, the tedious clinical virus detection can be made more simple.

3.2. Electrical testing methods

3.2.1. Electrochemical testing methods

Electrochemically, the utilization of gold (Au) or silver (Ag) nanoparticles modified electrodes will improve the performance of point-of-care testing (POCT) according to a study conducted by Ref. [71]. As an illustration, in the conductive mode, carbon nanotubes that were altered with Au/iron oxide magnetic nanoparticles were further modified with an electrode. This electrode had a LOD of 8.4 pM for hybrid DNA formed by the combination of IVA DNA and probe DNA [72]. Silk screen printed carbon electrode iPOCT modified

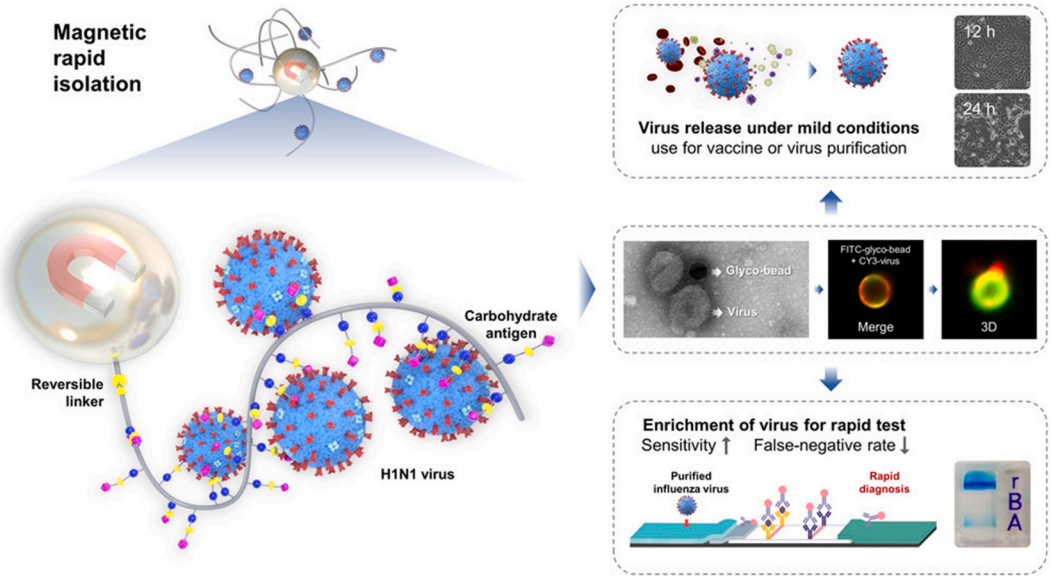

Fig. 2.

by boron nitride QDs/floral Au nanoparticles-antisense DNA oligonucleotides specifically detected SARS-CoV-2 RNA. The advantage of this method is that no nucleic acid amplification is required. Its sensitivity and specificity were 100 % and the LODs were lower than or comparable to RT-PCR [73] (Fig. 3A). A nano-electrochemical technique by adsorption of Ag nanoparticles onto the virus surface demonstrated an ideal method to trace a single IVA. An exceeding LOD (0.79 fM in PBS) was realized via an impedimetric immune POCT with Abs on a screen-printed carbon electrode (A. A. [74]). Another amplification strategy depends on quadruplex based on Au nanoparticles via (i) graphene, (ii) hybridization chain formation, (iii) hemin/G-quadruplex DNAzyme linkers, and (iv) alcohol dehydrogenase for H7N9 detection. Differential pulse voltammetry associated with H7N9 (8–60 pg center dot mL^{-1}) suggested a LOD of 0.81 pg center dot mL^{-1} (J. [75]).

For multi-target analysis, H5N1 and H1N1 can be detected on an electrochemical dual-POCT platform. Differential pulse voltammetry signals have a good correlation in the 25–500 pM range. The immune electrode amplified current sensitivity at the picomole level. In 1 min, the LOD was found to be 9.4 pM for H5N1 and H1N1 (M. [76]). An 8-channel electrochemical immunoassay platform for the detection of SARSCoV-2 and IVA (H1N1) suggested a lower false positive rate (5.4 %) than ELISA (40.5 %) [77].To estimate the graft density and virus detection mechanism of molecular recognition systems on different electrodes, molecular dynamics and density functional theory were used. When an antibody against SARS-CoV-2 binds to a nuclear protein, the impedance of electrochemical POCT is changed and recorded. With real clinical samples, this protocol allowed for a fast (<10 min) and LODs 0.362 (Au surfaces), 0.334 (boron-doped diamond), and 0.227 (glassy carbon) ng mL^{-1} [78] (Fig. 3 B).

3.2.2. *Electrode testing methods*

Electrode is a developing method for Point-of-Care Testing (POCT) of IVs. Electrolyte-gated organic field-effect transistors, similar to an electronic tongue, rely on the doctor blading and Langmuir-Schaefer approach. These transistors provide excellent consistency when testing IVA.The strain H7N1 (E. Y. [79]).

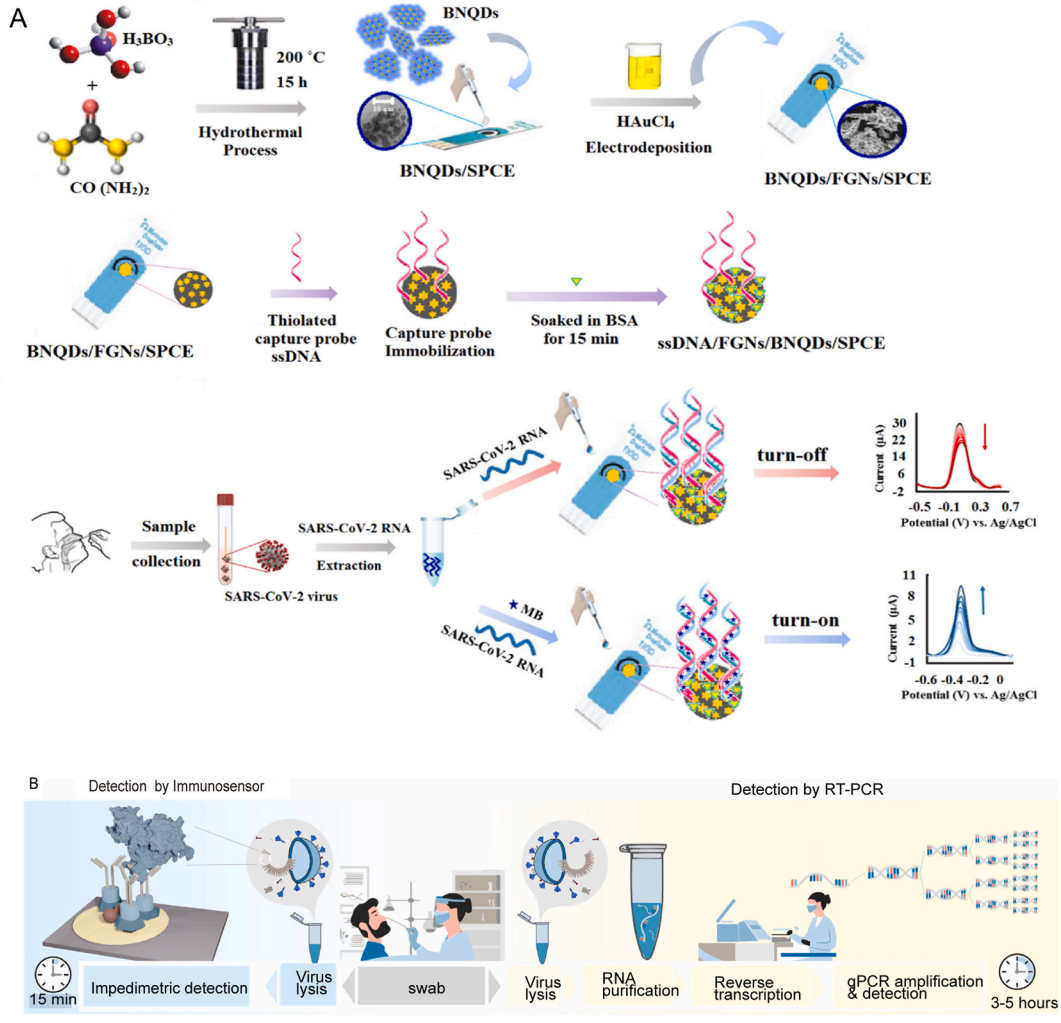

Fig. 3.

Nickel-reduced GO/MXene nanocomposites/glassy carbon electrodes (GCE) was used to prepare an ultra-sensitive peptide-based POCT for the detection of H1N1 and H5N2 (Y. V. [80]). The virus deposited on the electrode, and the NiO-rGO/MXene nanocomposite produced a synergistic signaling effect. The detection limits for H1N1 and H5N1 were 3.63 nM and 2.39 nM in artificial human blood plasma, respectively. The capacitive immuno POCT was able to detect the virus quickly and achieve a lower detection limit (0.25 pg mL^{-1}) (C. [81]), which is 6 levels lower than previous methods. The virus was attracted to the electrode by alternating current. Isolating and amplifying nucleotides increased the LOD and shortened the detection time (30 s), along with high sensitivity (90 %) and specificity (70 %).

3.2.3. Electrochemiluminescent testing methods

Electrochemiluminescent POCT has been advantages of unique sensitivity and low cost. For example, electrochemiluminescence serology POCT for quantitation of SARSCoV-2 showed satisfied precision (10.2%–15.1 %), recovery (107%–118 %), selectivity (102%–104 %), and reproducibility (0.89–1.18 overall fold difference) (D. [82]). SARS-CoV-2 spike antigen, receptor binding domain antigen, and nucleocapsid antigen were determined at 7, 13 and 7 arbitrary units mL^{-1}, respectively. The clinical sensitivity was 100 %, 98.8 % and 84.9 %. It was consistent (≥87.7 %) by comparison with the commercial method (Elecsys®). For high-throughput detection, an electrochemiluminescent POCT realized a detection of 19 strains of H1N1 and H3N2 IVs within 1 h (X. H. [83]). The method detected glucose with an electric current, in accordance with IVs or its enzymes. The detection limits and ranges are 10^2 and 10^2-10^8 plaques forming units, respectively.

The sensitivity of electrical technology can improve the sensitivity of virus detection. The lower detection limit makes it possible to detect even small amounts of the virus in the sample, which is also a much-needed technology for clinical testing.

3.3. Lateral flow and vertical flow testing methods

Lateral flow assay (LFA) provides a rapid IVAs screening method. Among diversified labels, Au nanoparticles and fluorescence nanomaterials provide satisfied performance (P. [84]). Yasufumi Matsumura and coworkers (Y. [85]) developed Au or Pt latex nanoparticles for assaying IVA H1N1 antigen at 6.25×10^{-3} (Au) and 2.5×10^{-2} (Pt NP-latex) HAU mL^{-1}.

Another method used Ab@CdSe/CdS/ZnS QD@latex in detecting IVA H1N1 or H3N2. As to IVA H1N1, the sensitivity (2.5 HAU mL^{-1}) was one order higher than that of an Eu-fluorescent immunochromatographic test (FICT) and a rapid diagnostic test (RDA). One or two orders higher sensitivity (0.63 HAU mL^{-1}) was recorded when compared with Eu-FICT and RDA for IVA H3N2.

Upon analysis of clinical nasopharyngeal swab specimens, the results indicated a clinical sensitivity of 93.75 %, clinical specificity of 100 %, and a kappa value of 0.98 when compared to real-time RT-PCR (A. V. T. [86]). Instead, a carbon nanotag similar to nano strings demonstrated a clear limit of detection (LOD) of 350 TCID50 mL^{-1} in allantoic fluid when used to identify the inoculation allantoic fluid containing H1N1 and H3N2 viruses, with minimal interference (N. [87]).

In terms of shortening detection time, on poly (ether sulfone) substrate, Rodriguez et al. (N. M. [88]) developed an LFA for IVA H1N1 detection in clinical nasopharyngeal specimens within 45 min, without sample preparation. The paper matrix integrated RNA extraction and purification, in situ isothermal amplification, and detection, providing a 10-fold improved LOD (10^6 copies mL^{-1}) than immunoassays. Testing directly on the strip can greatly reduce the time. For example, SARS-CoV-2 nucleocapsid protein was integrated into a paper vertical flow, allowing short detection time of only 10 min (S. [89]). The test achieved LODs of 40 pM in mock swab.

For high-throughput detection, a lateral flow with dual recognition element has been developed as a POCT platform to improve virus detection specificity by pairing nucleic aptamers with antibodies. It can distinguish IVs types and subtypes. Compared to qRT-PCR, this method showed a good accuracy (consistently over 90 %) [90]. A dual-mode single lateral flow assay strip was developed for detecting SARS-CoV-2 and IVA simultaneously. This proposal reduced the false-negative rate compared to the commercial colorimetric lateral flow method [91].

The application of Lateral flow and vertical flow makes clinical virus detection possible in non-laboratory Settings, such as at home. It not only promotes the commercialization of virus detection technology, but also makes virus detection more user-friendly.

3.4. Minimized testing methods

3.4.1. Microfluidics testing methods

Microfluidics or nanofluidics provide diversified formats for IVs detection, especially integrated with magneto fluidics for self-driving (A. Y. [92]), nano templating fluidic (T. [93]). A self-driven microfluidic device integrated RNA isolation and lysis via H1N1 aptamer@magnetic beads, as well as LAMP and colorimetric detection within 40 min, resulting in LOD of 3×10^{-4} HAU $reaction^{-1}$. The application of capillary forces through a PDMS surface via hydrophobic soft valves reduced the power consumption, compared to vibration-type liquid micromixers on microfluidic devices. The operation procedure was simplified by using a micromixer with a higher mixing index of 85 % within 1 s, five times higher than that of a pneumatically driven micromixer (17 %) [94]. Three-dimensional (3D) nano-templating fluidic devices can be used to capture fluorescent probes by fixing polymers at specific locations, realizing the simultaneous detection of multiple IVs (SARS-CoV-2 and IVA) with high specificity and high sensitivity (T. [93]).

The detection time for IAV H1N1 using digital structure-free microfluidics was 40 min. This method relied on the detection of single aptamer/double antibodies using magnetic beads. The droplets were conveyed, blended, removed, and positioned without requiring a microstructure, propelled by electromagnetic forces. The measured limit of detection (LOD) was 0.032 HAU, with a range spanning from 32 to 3.2 × 10-3 HAU. This range is 30 times less than that of serological tests and commercial RIDTs. Ultimately, a throat swab with a standard sample revealed the presence of 3.2 HUA (P. H. [95]). A “sliding" test based on asymmetric immune aggregation was

applied to detect IVA (H1N1) nuclear protein (54 pg mL^{-1}-54 ng mL^{-1}) in 10 min (S. [96]). H1N1 virus concentration can be calculated using a program code with a LOD of 40 pg mL^{-1} by the movement of asymmetric immune aggregation beads on the surface of the microchannel.

The formats are applied in IVA detection, such as lab-on-a-disc and chip. Major work focused on reduced operation, detecting time, and regent consumption. First, to reduce the error-causing manual operation, the automation, including pre-loading, lysis, extraction, and purification of RNA, as well as specific RNA detection with real-RT-LAMP, can be achieved by using membrane-resistance (MembR) valves under 5 different rotational speeds. The automated microdevice is built on a laboratory disc with MembR valves and can complete the test in 70 min with sensitivity as low as 25 times (Q. [97]). As an alternative format, high-throughput and highly sensitive multiplexed ultrasensitive sample-to-answer LAMP (MUSAL) have been assembled to take advantage of the photothermal amplification properties of LEDs, enabling simultaneously tracing of six SARS-CoV-2 and IVs with a detection limit of 0.5 times μL^{-1} [98] (Fig. 4).

Compared with the limited slots in LFA, microfluidic POCT can provide more flexible ways to improve the signal value and detection throughput. Enzyme and chromogenic substrates were to amplify visible signals. This proposal demonstrated a 70 % level of accuracy when compared to the results obtained from qRT-PCR. The proportion of legitimate completed device runs that met the required criteria was 92 %, and the negative predictive value for IVA and IVB was 81 %. Sample handling is facilitated by magnetism, and the identification of many Influenza A virus strains (H1N1, H3N2, H9N2) was successfully accomplished using nucleic acid hybridization on microfluidics (R. Q. [99]). Another example integrated magnetic beads pre-treatment and LAMP for signal enhancement in an eight-channel microfluidic array for six IVs by real-time colorimetry [100]. In order to minimize the presence of aerosol contamination, the process involved enclosing the sample collection and preparation, nucleic acid extraction using magnetic beads, in situ detection, and signal output within a sealed chip, all completed within a time frame of 1 h. Testing 109 clinical samples demonstrated a specificity of 100 % and a sensitivity of 96 %. The LODs were from 10 to 100 fg per microliter (fg μL^{-1}), which were up to 100 times superior to those of polymerase chain reaction (PCR). The primary obstacle in the detection of multiple IVs using microfluidics is the extended duration required, often ranging from 60 to 80 min. In order to address the issue, a reduced testing duration of 20 min was observed using a combined PDMS/Si microfluidic device for the simultaneous identification of three influenza viruses (IVA H1N1, H3N2, IVB). This was achieved by leveraging the binding properties of a universal aptamer against the aforementioned viruses (C. H. [101]).

3.4.2. *Microarray (spot)-based testing methods*

The colorimetric ELISA sensitivity can be improved via a microarray, microplate, or microwell than commercial kits (H. O. [102]). A polydiacetylene-based colorimetric microplate was established to detect IVA H1N1 with naked eyes and smartphone by color change. On a polyvinylidene fluoride membrane, the antibody against IVA H1N1 were pre-conjugated into this polydiacetylene by photopolymerization. The microplate posed a color change from blue to red depending on temperature and pH values. After the H1N1 antigen was specifically recognized by anti-hemagglutinin antibody and enriched by nanobeads, the Au nanozymes were used as the peroxidase-like artificial catalyst. LODs were 5.0×10^{-12} and 44.2×10^{-15} g mL^{-1} by eyes and commercial microreader, respectively, along with linearity of 5.0×10^{-15}-5.0×10^{-6} g mL^{-1} (S. U. [103]).

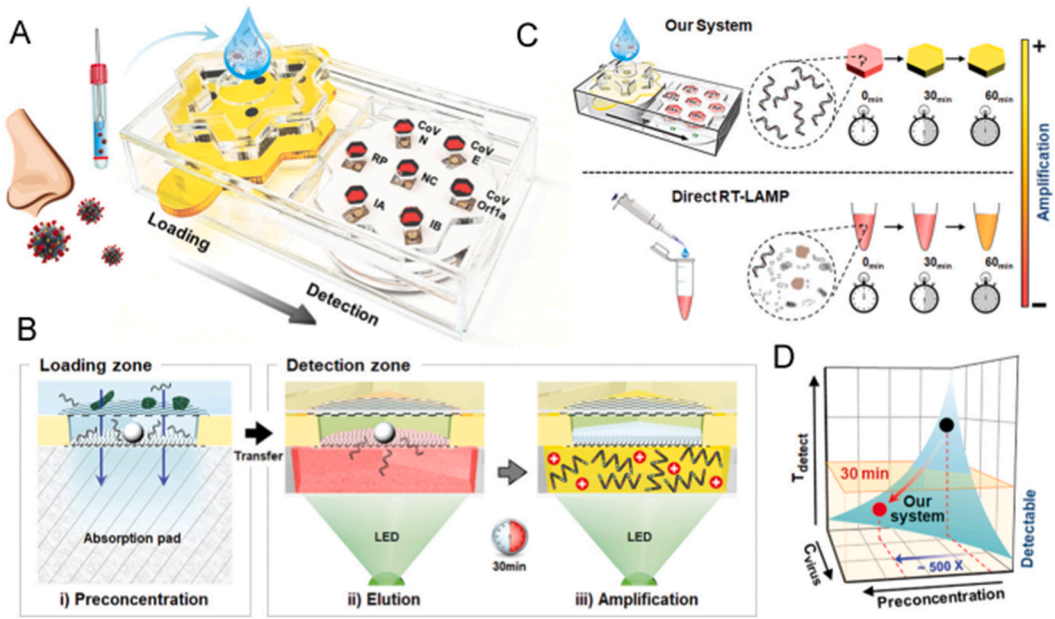

Fig. 4.

A single digital virus immunoassay via microarray was developed (Z. [104]) by using multi-functional QD@Fe_2O_3@nanospheres with green, yellow, and red emission wavelengths. The Fe_2O_3 separated targets without sample pre-treatment to realize the detection of H9N2, H1N1, and H7N9 via a sandwich immunoreaction, where the micropores with or without fluorescence were denoted as "1″ or "0″, respectively. Due to excellent photostability and resolvable fluorescence of QDs nanospheres, the LOD is as low as 0.02 pg mL^{-1}.

The miniaturization of virus detection equipment, while reducing costs, also enables a wider range of new technologies to be combined. It has promoted the development of the field academically and improved the working mode clinically.

4. Emerging testing methods

4.1. Smartphone-based testing methods

The advent of smartphone affords a portable iPOCT format for IAV detection (D. M. [105], P. [106]), usually assisted with microfludics (Y. Q. [107]).

A smartphone mobile imaging for digital counting of H1N1 was reported for the low noise fluorescence imaging (Y. [108]). In a 23 × 10 × 7 cm (length × width × height) microdevice, an evanescent field illumination resulted from incident light via a riser reactor array device, realizing fluorescence detect a single IVA from riser reactors. The detection efficiency was 60 %, two orders better than commercial IV tests. The low detection efficiency attributed low S/N ratio compared with microscopy and the inevitable inherent heterogeneity of neuraminidase activity among virus particles.

The functional gold cluster is highly sensitive to SARS-CoV-2 test, and the LOD in human saliva is 0.28 PFU mL^{-1}. Combined with the smartphone camera and the application to process the image, the computer algorithm can get 100 % accuracy, and the process response speed, the biggest advantage is the small sample size (20 μL) (E. M. [109]) (Fig. 5). Colorimetric ring-mediated LAMP binding can reduce LODs. For example, Yu-Dong Ma et al .[110] developed a smartphone-enabled, passive, self-actuated microfluidics for detecting IVA H1N1 in 40 min. This proposal integrated purification via aptamer@magnetic beads, low-temperature lysis of viruses, LAMP, and quantification via colorimetric sensors. Based on the punch-press mechanism, the smartphone controls and monitors the entire detection process with a LOD of 0.0032HAU.

4.2. Pressure-based testing methods

After antibody-antigen recognition, platinum-induced catalysis can generate gas. The gas pressure can be recorded by a portable gas reader for quantitation of virus, which had a sensitivity compared to ELISA. The stability of Pt nanoparticles decorated antibodies and nonspecific adsorption of Pt nanoparticles need to be comprehensively considered (L. [111]).

The superior application technology of smart phones, such as high-definition cameras, real-time cloud platform transmission, etc., is combined with the clinical detection of viruses. The results can be shared, stored for a long time and updated in time. This is not only a reform in the field of virus detection, but also to promote the development of the industry in a new direction of intelligence.

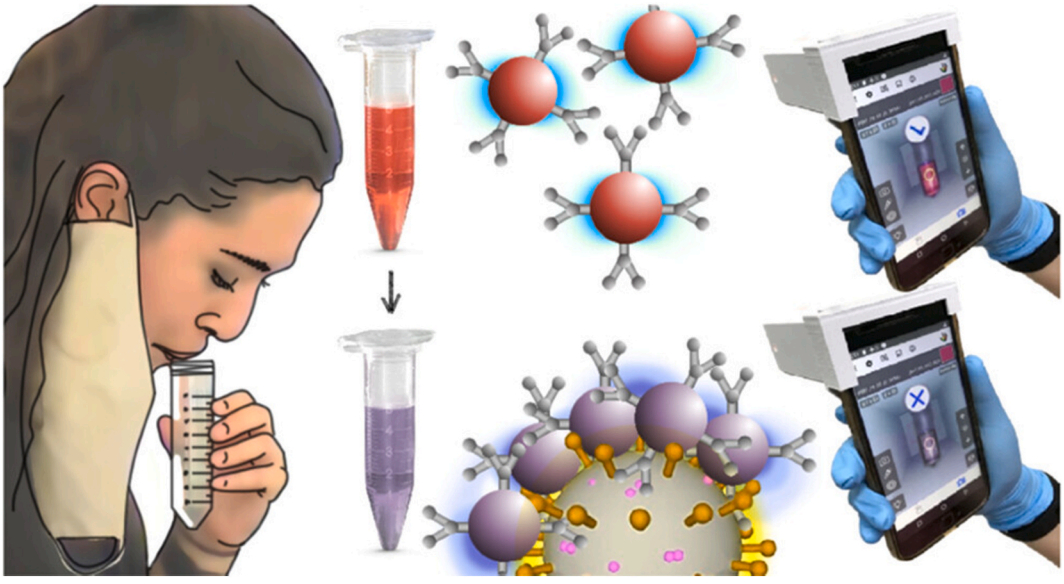

Fig. 5.

5. Conclusion

Emerging IVs-induced pandemics cause huge healthcare burdens and economic losses. Rapid diagnosis via POCT will effectively limit IVs spread. POCT for IVs has been challenging because of the recognition format, signal amplification, complex matrices, and distinguishing between live viruses or others. These issues are expected to be addressed in the design of POCT for IV systems. The recognition format is determined by the morpho-structure of nucleic acid, antigen-antibody, or aptamer. Independent variables. Some genes or mutations change annually, necessitating the development of more efficient and precise recognition formats. Furthermore, promptly detecting IV in its first phase can be crucial in terms of both time and life-saving, as it allows for the implementation of appropriate interventions and medications. Thus, it is essential to develop high sensitive POCT method to test single IV particles. Signal amplification is requested in the high sensitive POCT. Although sparking signal amplification strategies have been investigated, for the real application, stable and reliable signal amplification is rarely reported. Third, complex matrices can induce fake positive or negative. In order to address the matric effect, it is necessary to conduct a thorough investigation and comparison of more resilient sample preparation methods in clinical laboratories. Furthermore, distinguishing between live IVs and dead viruses poses a common challenge that necessitates the use of improved POCT.

Diversified POCT formats have been well introduced, like nucleic acid amplification, optical POCT, test strips, microfluidics, microarray, allowing IVs testing from practical clinical settings to self-diagnosis at home. However, commercialized POCT for IVs are limited, with the unsatisfied sensitivity and specificity. A comprehensive evaluation of POCT methods and products should be done to establish a standardized benchmark for comparison with normal IVs tests. This would facilitate the widespread use of POCT methods and products worldwide. Challenges of commercialized POCT for IVs include high precision, sensitivity, specificity, standardization by the international authorities, certification between countries, test processing simplification, and cost in source-limited settings.

The future prospects for point-of-care testing (POCT) for IV applications are promising, with potential for widespread use in both developed and developing regions, particularly in resource-constrained settings. This review aims to provide an overview of Point-of-Care Testing (POCT) for IV procedures, covering the scientific background and practical applications. The ultimate goal is to enhance the diagnostic capabilities and alleviate the challenges faced by IVs.

Data availability statement

Data openly available in a public repository.

CRediT authorship contribution statement

Le Zhang: Writing – original draft. **Chunwen Li:** Writing – original draft. **ShaSha Shao:** Formal analysis. **Zhaowei Zhang:** Writing – review & editing. **Di Chen:** Project administration, Funding acquisition, Conceptualization.

Declaration of generative AI and AI-assisted technologies in the writing process

There is nothing to disclose.

Declaration of competing interest

The authors have no conflicts of interest to declare.

Acknowledgments

The authors thanks to the Natural Science Foundation of Hubei Province (2020CFB731).

Le Zhang is a Ph.D candiate in School of Ecology and Environment at Tibet University, and co-trained at Huazhong University of Science and Technology.

References

[1] A. Ismail, et al., Aflatoxin in foodstuffs: occurrence and recent advances in decontamination, Food Res. Int. 113 (2018) 74–85, https://doi.org/10.1016/j.foodres.2018.06.067.
[2] N.J. Roberts Jr., L.R. Krilov, The continued threat of influenza A viruses, Viruses-Basel 14 (5) (2022), https://doi.org/10.3390/v14050883.
[3] T.M. Uyeki, et al., Influenza, Lancet 400 (10353) (2022) 693–706, https://doi.org/10.1016/S0140-6736(22)00982-5.
[4] S.N. Bevins, et al., Intercontinental movement of highly pathogenic avian influenza A(H5N1) clade 2.3.4.4 virus to the United States, 2021, Emerg. Infect. Dis. 28 (5) (2022) 1006–1011, https://doi.org/10.3201/eid2805.220218.
[5] J.M. Rijks, et al., Mass mortality caused by highly pathogenic influenza A(H5N1) virus in sandwich terns, The Netherlands, 2022, Emerg. Infect. Dis. 28 (12) (2022) 2538–2542, https://doi.org/10.3201/eid2812.221292.
[6] W. Sun, et al., Cross-species infection potential of avian influenza H13 viruses isolated from wild aquatic birds to poultry and mammals, Emerg. Microb. Infect. (2023) 2184177, https://doi.org/10.1080/22221751.2023.2184177, 2184177.
[7] U. Molini, et al., First influenza D virus full-genome sequence retrieved from livestock in Namibia, Africa, Acta Trop. 232 (2022), https://doi.org/10.1016/j.actatropica.2022.106482.
[8] M.W. Brand, et al., Bivalent hemagglutinin and neuraminidase influenza replicon particle vaccines protect pigs against influenza a virus without causing vaccine associated enhanced respiratory disease, Vaccine 40 (38) (2022) 5569–5578, https://doi.org/10.1016/j.vaccine.2022.07.042.

[9] R.P. Chauhan, M.L. Gordon, Review of genome sequencing technologies in molecular characterization of influenza A viruses in swine, J. Vet. Diagn. Invest. 34 (2) (2022) 177–189, https://doi.org/10.1177/10406387211068023.

[10] K.A. Ciuoderis, et al., Use of oral fluids for efficient monitoring of influenza viruses in swine herds in Colombia, Rev. Colombiana Ciencias Pecuarias 35 (3) (2022) 141–152, https://doi.org/10.17533/udea.rccp.v35n3a02.

[11] G. Lopez-Moreno, et al., Evaluation of internal farm biosecurity measures combined with sow vaccination to prevent influenza A virus infection in groups of due-to-wean pigs, BMC Vet. Res. 18 (1) (2022), https://doi.org/10.1186/s12917-022-03494-z.

[12] M.A. De Marco, et al., Long-term serological investigations of influenza A virus in free-living wild boars (sus scrofa) from northern Italy (2007-2014), Microorganisms 10 (9) (2022), https://doi.org/10.3390/microorganisms10091768.

[13] T.M. Chambers, Equine influenza, Cold Spring Harb. Perspect. Med. 12 (1) (2022), https://doi.org/10.1101/cshperspect.a038331.

[14] J.T.L. Cheung, et al., Determining existing human population immunity as part of assessing influenza pandemic risk, Emerg. Infect. Dis. 28 (5) (2022) 977–985, https://doi.org/10.3201/eid2805.211965.

[15] L. Zhang, Clinical features of the first critical case of acute encephalitis caused by the avian influenza A (H5N6) virus, Emerg. Microb. Infect. 11 (1) (2022) 2437–2446, https://doi.org/10.1080/22221751.2022.2122584.

[16] L. Laloli, et al., Time-resolved characterization of the innate immune response in the respiratory epithelium of human, porcine, and bovine during influenza virus infection, Front. Immunol. 13 (2022), https://doi.org/10.3389/fimmu.2022.970325.

[17] S. Renu, et al., Gut microbiota of obese children influences inflammatory mucosal immune pathways in the respiratory tract to influenza virus infection: optimization of an ideal duration of microbial colonization in a gnotobiotic pig model, Microbiol. Spectr. 10 (3) (2022), https://doi.org/10.1128/spectrum.02674-21.

[18] P. Wang, et al., Impact of COVID-19 pandemic on influenza virus prevalence in children in Sichuan, China, J. Med. Virol. 95 (1) (2023), https://doi.org/10.1002/jmv.28204.

[19] G. Hoy, et al., The spectrum of influenza in children, Clin. Infect. Dis. (2022), https://doi.org/10.1093/cid/ciac734.

[20] K. Dziąbowska, et al., Detection methods of human and animal influenza virus—current trends, Biosensors 8 (4) (2018), https://doi.org/10.3390/bios8040094.

[21] S. Bangaru, et al., A multifunctional human monoclonal neutralizing antibody that targets a unique conserved epitope on influenza HA, Nat. Commun. 9 (2018), https://doi.org/10.1038/s41467-018-04704-9.

[22] Z.W. Zhang, Advanced point-of-care testing technologies for human acute respiratory virus detection, Adv. Mater. 34 (1) (2022), https://doi.org/10.1002/adma.202103646.

[23] W. Teixeira, et al., An all-in-one point-of-care testing device for multiplexed detection of respiratory infections, Biosens. Bioelectron. 213 (2022), https://doi.org/10.1016/j.bios.2022.114454.

[24] G.F. Li, Influenza virus precision diagnosis and continuous purification enabled by neuraminidase-resistant glycopolymer-coated microbeads, ACS Appl. Mater. Interfaces 13 (39) (2021) 46260–46269, https://doi.org/10.1021/acsami.1c11561.

[25] T. Zheng, et al., Specific lateral flow detection of isothermal nucleic acid amplicons for accurate point-of-care testing, Biosens. Bioelectron. 222 (2023) 114989, https://doi.org/10.1016/j.bios.2022.114989, 114989.

[26] T. Hasegawa, et al., Quantitative performance of digital ELISA for the highly sensitive quantification of viral proteins and influenza virus, Anal. Bioanal. Chem. 415 (10) (2023) 1897–1904, https://doi.org/10.1007/s00216-023-04600-2.

[27] Z. Fattahi, M. Hasanzadeh, Nanotechnology-assisted microfluidic systems for chemical sensing, biosensing, and bioanalysis, Trac-Trend. Anal. Chem. (2022) 152, https://doi.org/10.1016/j.trac.2022.116637.

[28] M. Xiao, et al., Virus detection: from state-of-the-art laboratories to smartphone-based point-of-care testing, Adv. Sci. 9 (17) (2022) e2105904, https://doi.org/10.1002/advs.202105904.

[29] M. Ogrzewalska, et al., Influenza A(H11N2) virus detection in fecal samples from adelie (pygoscelis adeliae) and chinstrap (pygoscelis antarcticus) penguins, penguin island, Antarctica, Microbiol. Spectr. (2022), https://doi.org/10.1128/spectrum.01427-22.

[30] F. Yang, A multiplex real-time RT-PCR method for detecting H5, H7 and H9 subtype avian influenza viruses in field and clinical samples, Virus Res. 309 (2022) 198669, https://doi.org/10.1016/j.virusres.2021.198669.

[31] L. Chen, et al., Performance of the cobas(®) influenza A/B assay for rapid pcr-based detection of influenza compared to prodesse proflu+ and viral culture, Eur. J. Immunol. 5 (4) (2015) 236–245, https://doi.org/10.1556/1886.2015.00046.

[32] S. Young, et al., Diagnostic accuracy of the real-time PCR cobas® Liat® Influenza A/B assay and the Alere i Influenza A&B NEAR isothermal nucleic acid amplification assay for the detection of influenza using adult nasopharyngeal specimens, J. Virol. 94 (2017) 86–90, https://doi.org/10.1016/j.jcv.2017.07.012.

[33] R.R.G. Soares, et al., Silica bead-based microfluidic device with integrated photodiodes for the rapid capture and detection of rolling circle amplification products in the femtomolar range, Biosens. Bioelectron. 128 (2019) 68–75, https://doi.org/10.1016/j.bios.2018.12.004.

[34] Z. Yang, et al., Detection of the pandemic H1N1/2009 influenza A virus by a highly sensitive quantitative real-time reverse-transcription polymerase chain reaction assay, Virol. Sin. 28 (1) (2013) 24–35, https://doi.org/10.1007/s12250-013-3290-0.

[35] L.M. Howard, et al., A novel real-time RT-PCR assay for influenza C tested in Peruvian children, J. Virol. 96 (2017) 12–16, https://doi.org/10.1016/j.jcv.2017.08.014.

[36] M.J. Binnicker, et al., Direct detection of influenza A and B viruses in less than 20 minutes using a commercially available rapid PCR assay, J. Clin. Microbiol. 53 (7) (2015) 2353–2354, https://doi.org/10.1128/jcm.00791-15.

[37] N.E. Babady, et al., Multicenter evaluation of the ePlex respiratory pathogen panel for the detection of viral and bacterial respiratory tract pathogens in nasopharyngeal swabs, J. Clin. Microbiol. 56 (2) (2018), https://doi.org/10.1128/jcm.01658-17.

[38] Y. Song, Charge-shifting polyplex as a viral RNA extraction carrier for streamlined detection of infectious viruses, Mater. Horiz. 10 (10) (2023) 4571–4580, https://doi.org/10.1039/d3mh00861d.

[39] Z.J. Gu, et al., Bead-based multiplexed droplet digital polymerase chain reaction in a single tube using universal sequences: an ultrasensitive, cross-reaction-free, and high-throughput strategy, ACS Sens. 7 (9) (2022) 2759–2766, https://doi.org/10.1021/acssensors.2c01415.

[40] P. McMullen, et al., The performance of Luminex ARIES (R) Flu A/B & RSV and Cepheid Xpert (R) Flu/RSV XC for the detection of influenza A, influenza B, and respiratory syncytial virus in prospective patient samples, J. Virol. 95 (2017) 84–85, https://doi.org/10.1016/j.jcv.2017.08.018.

[41] P. Khan, et al., Isothermal SARS-CoV-2 diagnostics: tools for enabling distributed pandemic testing as a means of supporting safe reopenings, ACS Synth. Biol. 9 (11) (2020) 2861–2880, https://doi.org/10.1021/acssynbio.0c00359.

[42] M. Clementino, et al., Detection of SARS-CoV-2 in different human biofluids using the loop-mediated isothermal amplification assay: a prospective diagnostic study in Fortaleza, Brazil, J. Med. Virol. 94 (9) (2022) 4170–4180, https://doi.org/10.1002/jmv.27842.

[43] S.Y. Wang, et al., Amine-functionalized quantum dots as a universal fluorescent nanoprobe for a one-step loop-mediated isothermal amplification assay with single-copy sensitivity, ACS Appl. Mater. Interfaces 14 (31) (2022) 35299–35308, https://doi.org/10.1021/acsami.2c0250835299.

[44] S. Banerjee, et al., Piecewise isothermal nucleic acid testing (PINAT) for infectious disease detection with sample-to-result integration at the point-of-care, ACS Sens. 6 (10) (2021) 3753–3764, https://doi.org/10.1021/acssensors.1c01573.

[45] T.L. Quyen, et al., Multiplexed detection of pathogens using solid-phase loop-mediated isothermal amplification on a supercritical angle fluorescence array for point-of-care applications, ACS Sens. 7 (11) (2022) 3343–3351, https://doi.org/10.1021/acssensors.2c01337.

[46] W.I. Lee, et al., Potentiometric biosensors based on molecular-imprinted self-assembled monolayer films for rapid detection of influenza A virus and SARS-CoV-2 spike protein, ACS Appl. Mater. Interfaces 5 (4) (2022) 5045–5055, https://doi.org/10.1021/acsanm.2c00068.

[47] D. Lee, et al., Point-of-Care toolkit for multiplex molecular diagnosis of SARS-CoV-2 and influenza A and B viruses, ACS Sens. 6 (9) (2021) 3204–3213, https://doi.org/10.1021/acssensors.1c00702.

[48] J. Yang, RT-LAMP assay for rapid detection of the R203M mutation in SARS-CoV-2 Delta variant, Emerg. Microb. Infect. 11 (1) (2022) 978–987, https://doi.org/10.1080/22221751.2022.2054368.

[49] J.H. Jung, et al., Integrated centrifugal reverse transcriptase loop-mediated isothermal amplification microdevice for influenza A virus detection, Biosens. Bioelectron. 68 (2015) 218–224, https://doi.org/10.1016/j.bios.2014.12.043.

[50] X. Ye, et al., Argonaute-integrated isothermal amplification for rapid, portable, multiplex detection of SARS-CoV-2 and influenza viruses, Biosens. Bioelectron. 207 (2022) 114169, https://doi.org/10.1016/j.bios.2022.114169.

[51] K. Yoshimi, et al., CRISPR-Cas3-based diagnostics for SARS-CoV-2 and influenza virus, iScience 25 (2) (2022), https://doi.org/10.1016/j.isci.2022.103830.

[52] H. Zhou, et al., CRISPR/Cas13a combined with hybridization chain reaction for visual detection of influenza A (H1N1) virus, Anal. Bioanal. Chem. 414 (29–30) (2022) 8437–8445, https://doi.org/10.1007/s00216-022-04380-1.

[53] B.J. Park, et al., Specific detection of influenza A and B viruses by CRISPR-cas12a-based assay, Biosensors 11 (3) (2021), https://doi.org/10.3390/bios11030088.

[54] N. Lee, User-friendly point-of-care detection of influenza A (H1N1) virus using light guide in three-dimensional photonic crystal, RSC Adv. 8 (41) (2018) 22991–22997, https://doi.org/10.1039/c8ra02596g.

[55] M.K. Tsang, et al., Upconversion luminescence sandwich assay for detection of influenza H7 subtype, Adv. Funct. Mater. 8 (18) (2019), https://doi.org/10.1002/adhm.201900575.

[56] G.L. Liu, et al., Silver nanoclusters beacon as stimuli-responsive versatile platform for multiplex DNAs detection and aptamer- substrate complexes sensing, Anal. Chim. 89 (1) (2017) 1002–1008, https://doi.org/10.1021/acs.analchem.6b04362.

[57] N. Kumar, et al., Label-free peptide nucleic acid biosensor for visual detection of multiple strains of influenza A virus suitable for field applications, Anal. Chim. Acta 1093 (2020) 123–130, https://doi.org/10.1016/j.aca.2019.09.060.

[58] S.R. Ahmed, et al., Self-assembled star-shaped chiroplasmonic gold nanoparticles for an ultrasensitive chiro-immunosensor for viruses, RSC Adv. 7 (65) (2017) 40849–40857, https://doi.org/10.1039/c7ra07175b.

[59] M. B., Mechanisms of influenza virus HA2 peptide interaction with liposomes studied by dual-wavelength MP-SPR, ACS Appl. Mater. Interfaces 14 (29) (2022) 32970–32981, https://doi.org/10.1021/acsami.2c09039.

[60] P. Moitra, et al., Selective naked eye detection of SARS CoV 2 mediated by N gene targeted antisense oligonucleotide capped plasmonic nanoparticles, ACS Nano 14 (6) (2020) 7617–7627, https://doi.org/10.1021/acsnano.0c03822.

[61] K. Takemura, et al., Versatility of a localized surface plasmon resonance-based gold nanoparticle-alloyed quantum dot nanobiosensor for immunofluorescence detection of viruses, Biosens. Bioelectron. 89 (2017) 998–1005, https://doi.org/10.1016/j.bios.2016.10.045.

[62] I. Jung, et al., Fourier transform surface plasmon resonance (FTSPR) with gyromagnetic plasmonic nanorods, Angew. Chem. Int. Ed. 57 (7) (2018) 1841–1845, https://doi.org/10.1002/anie.201710619.

[63] I. Jung, et al., Fourier transform surface plasmon resonance of nanodisks embedded in magnetic nanorods, Nano Lett. 18 (3) (2018) 1984–1992, https://doi.org/10.1021/acs.nanolett.7b05439.

[64] F. Nasrin, et al., Fluorometric virus detection platform using quantum dots-gold nanocomposites optimizing the linker length variation, Anal. Chim. Acta 1109 (2020) 148–157, https://doi.org/10.1016/j.aca.2020.02.039.

[65] C.W. Wang, et al., Magnetic SERS strip for sensitive and simultaneous detection of respiratory viruses, ACS Appl. Mater. Interfaces 11 (21) (2019) 19495–19505, https://doi.org/10.1021/acsami.9b03920.

[66] Z. Zhang, Rapid detection of viruses: based on silver nanoparticles modified with bromine ions and acetonitrile, Chem. Eng. J. 438 (2022) 135589, https://doi.org/10.1016/j.cej.2022.135589.

[67] H. Chen, et al., SERS-based dual-mode DNA aptasensors for rapid classification of SARS-CoV-2 and influenza A/H1N1 infection, Sensor. Actuator. B Chem. (2022) 355, https://doi.org/10.1016/j.snb.2021.131324.

[68] D. Zhang, et al., Rapid and ultrasensitive quantification of multiplex respiratory tract infection pathogen via lateral flow microarray based on SERS nanotags, Theranostics 9 (17) (2019) 4849–4859, https://doi.org/10.7150/thno.35824.

[69] Y. Yang, et al., Rapid and quantitative detection of respiratory viruses using surface-enhanced Raman spectroscopy and machine learning, Biosens. Bioelectron. 217 (2022) 114721, https://doi.org/10.1016/j.bios.2022.114721.

[70] Y. Wang, Highly sensitive and automated surface enhanced Raman scattering-based immunoassay for H5N1 detection with digital microfluidics, Anal. Chim. 90 (8) (2018) 5224–5231, https://doi.org/10.1021/acs.analchem.8b00002.

[71] Y.J. Yang, Single-nanoparticle collision electrochemistry biosensor based on an electrocatalytic strategy for highly sensitive and specific detection of H7N9 avian influenza virus, Anal. Chim. 94 (23) (2022), https://doi.org/10.1021/acs.analchem.2c00913.

[72] J. Lee, A multi-functional gold/iron-oxide nanoparticle-CNT hybrid nanomaterial as virus DNA sensing platform, Biosens. Bioelectron. 102 (2018) 425–431, https://doi.org/10.1016/j.bios.2017.11.052.

[73] B. Hatamluyi, et al., Sensitive and specific clinically diagnosis of SARS-CoV-2 employing a novel biosensor based on boron nitride quantum dots/flower-like gold nanostructures signal amplification, Biosens. Bioelectron. (2022) 207, https://doi.org/10.1016/j.bios.2022.114209.

[74] A.A. Dunajova, et al., Ultrasensitive impedimetric imunosensor for influenza A detection, J. Electroanal. Chem. 858 (2020), https://doi.org/10.1016/j.jelechem.2019.113813.

[75] J. Yang, et al., Quadruple signal amplification strategy based on hybridization chain reaction and an immunoelectrode modified with graphene sheets, a hemin/G-quadruplex DNAzyme concatamer, and alcohol dehydrogenase: ultrasensitive determination of influenza virus subtype H7N9, Microchim. Acta 182 (15–16) (2015) 2377–2385, https://doi.org/10.1007/s00604-015-1583-8.

[76] M. Veerapandian, et al., Dual immunosensor based on methylene blue-electroadsorbed graphene oxide for rapid detection of the influenza A virus antigen, Talanta 155 (2016) 250–257, https://doi.org/10.1016/j.talanta.2016.04.047.

[77] J. Li, Multichannel immunosensor platform for the rapid detection of SARS-CoV-2 and influenza A(H1N1) virus, ACS Appl. Mater. Interfaces 13 (19) (2021) 22262–22270, https://doi.org/10.1021/acsami.1c05770.

[78] W. Bialobrzeska, et al., Performance of electrochemical immunoassays for clinical diagnostics of SARS-CoV-2 based on selective nucleocapsid N protein detection: boron-doped diamond, gold and glassy carbon evaluation, Biosens. Bioelectron. 209 (2022), https://doi.org/10.1016/j.bios.2022.114222.

[79] E.Y. Poimanova, et al., Biorecognition layer based on biotin-containing 1 benzothieno 3,2-b 1 benzothiophene derivative for biosensing by electrolyte-gated organic field-effect transistors, ACS Appl. Mater. Interfaces 14 (14) (2022) 16462–16476, https://doi.org/10.1021/acsami.1c24109.

[80] Y.V. Manohara Reddy, et al., Fine-tuning of MXene-nickel oxide-reduced graphene oxide nanocomposite bioelectrode: sensor for the detection of influenza virus and viral protein, Biosens. Bioelectron. 214 (2022) 114511, https://doi.org/10.1016/j.bios.2022.114511.

[81] C. Cheng, et al., A PCR-free point-of-care capacitive immunoassay for influenza A virus, Microchim. Acta 184 (6) (2017) 1649–1657, https://doi.org/10.1007/s00604-017-2140-4.

[82] D. Wilkins, et al., Validation and performance of a multiplex serology assay to quantify antibody responses following SARS-CoV-2 infection or vaccination, Clin. Transl. Immunol. 11 (4) (2022) e1385, https://doi.org/10.1002/cti2.1385.

[83] X.H. Zhang, et al., Electrochemical assay to detect influenza viruses and measure drug susceptibility, Angew. Chem. Int. Ed. 54 (20) (2015) 5929–5932, https://doi.org/10.1002/anie.201412164.

[84] P. Sadeghi, et al., Lateral flow assays (LFA) as an alternative medical diagnosis method for detection of virus species: the intertwine of nanotechnology with sensing strategies, Trac-Trend. Anal. Chem. (2021) 145, https://doi.org/10.1016/j.trac.2021.116460.

[85] Y. Matsumura, et al., Metal (Au, Pt) nanoparticle-latex nanocomposites as probes for immunochromatographic test strips with enhanced sensitivity, ACS Appl. Mater. Interfaces 10 (38) (2018) 31977–31987, https://doi.org/10.1021/acsami.8b11745.

[86] A.V.T. Nguyen, et al., Sensitive detection of influenza a virus based on a CdSe/CdS/ZnS quantum dot-linked rapid fluorescent immunochromatographic test, Biosens. Bioelectron. 155 (2020), https://doi.org/10.1016/j.bios.2020.112090.

[87] N. Wiriyachaiporn, et al., Carbon nanotag based visual detection of influenza A virus by a lateral flow immunoassay, Microchim. Acta 184 (6) (2017) 1827–1835, https://doi.org/10.1007/s00604-017-2191-6.
[88] N.M. Rodriguez, et al., Paper-based RNA extraction, in situ isothermal amplification, and lateral flow detection for low-cost, aapid diagnosis of influenza A (H1N1) from clinical specimens, Anal. Chim. 87 (15) (2015) 7872–7879, https://doi.org/10.1021/acs.analchem.5b01594.
[89] S. Kim, et al., Developing a SARS-CoV-2 antigen test using engineered affinity proteins, ACS Appl. Mater. Interfaces 13 (33) (2021) 38990–39002, https://doi.org/10.1021/acsami.1c08174.
[90] T.T. Le, et al., Dual recognition element lateral flow assay toward multiplex strain specific influenza virus detection, Anal. Chim. 89 (12) (2017) 6781–6786, https://doi.org/10.1021/acs.analchem.7b01149.
[91] M. Lu, Dual-mode SERS-based lateral flow assay strips for simultaneous diagnosis of SARS-CoV-2 and influenza a virus, Nano Converg 9 (1) (2022), https://doi.org/10.1186/s40580-022-00330-w.
[92] A.Y. Trick, et al., Point-of-Care platform for rapid multiplexed detection of SARS-CoV-2 variants and respiratory pathogens, Adv. Mater. Technol. 7 (6) (2022), https://doi.org/10.1002/admt.202101013.
[93] T. Mortelmans, et al., Poly(methyl methacrylate)-based nanofluidic device for rapid and multiplexed serological antibody detection of SARS-CoV-2, ACS Appl. Mater. Interfaces 5 (1) (2022) 517–526, https://doi.org/10.1021/acsanm.1c03309.
[94] Y.D. Ma, A sample-to-answer, portable platform for rapid detection of pathogens with a smartphone interface, Lab Chip 19 (22) (2019) 3804–3814, https://doi.org/10.1039/c9lc00797k.
[95] P.H. Lu, et al., A structure-free digital microfluidic platform for detection of influenza a virus by using magnetic beads and electromagnetic forces, Lab Chip 20 (4) (2020) 789–797, https://doi.org/10.1039/c9lc01126a.
[96] S. Kim, et al., Asymmetric bead aggregation for microfluidic immunodetection, Lab Chip 17 (12) (2017) 2095–2103, https://doi.org/10.1039/c7lc00138j.
[97] Q. Liu, et al., A sample-to-answer labdisc platform integrated novel membrane-resistance valves for detection of highly pathogenic avian influenza viruses, Sens. Actuators B Chem. 270 (2018) 371–381, https://doi.org/10.1016/j.snb.2018.05.044.
[98] M. Song, Multiplexed ultrasensitive sample-to-answer RT-LAMP chip for the identification of SARS-CoV-2 and influenza viruses, Adv. Mater. (2023), https://doi.org/10.1002/adma.202207138.
[99] R.Q. Zhang, et al., Rapid detection and subtyping of multiple influenza viruses on a microfluidic chip integrated with controllable micro-magnetic field, Biosens. Bioelectron. 100 (2018) 348–354, https://doi.org/10.1016/j.bios.2017.08.048.
[100] R.L. Wang, Rapid detection of multiple respiratory viruses based on microfluidic isothermal amplification and a real-time colorimetric method, Lab Chip 18 (22) (2018) 3507–3515, https://doi.org/10.1039/c8lc00841h.
[101] C.H. Wang, et al., Integrated microfluidic device using a single universal aptamer to detect multiple types of influenza viruses, Biosens. Bioelectron. 86 (2016) 247–254, https://doi.org/10.1016/j.bios.2016.06.071.
[102] H.O. Kim, et al., Host cell mimic polymersomes for rapid detection of highly pathogenic influenza virus via a viral fusion and cell entry mechanism, Adv. Funct. Mater. 28 (34) (2018), https://doi.org/10.1002/adfm.201800960.
[103] S.U. Son, et al., Naked-eye detection of pandemic influenza a (pH1N1) virus by polydiacetylene (PDA)-based paper sensor as a point-of-care diagnostic platform, Sens. Actuators B Chem. 291 (2019) 257–265, https://doi.org/10.1016/j.snb.2019.04.081.
[104] Z. Wu, et al., Digital single virus immunoassay for ultrasensitive multiplex avian influenza virus detection based on fluorescent magnetic multifunctional nanospheres, ACS Appl. Mater. Interfaces 11 (6) (2019) 5762–5770, https://doi.org/10.1021/acsami.8b18898.
[105] D.M. Heithoff, et al., Assessment of a smartphone-based loop-mediated isothermal amplification assay for detection of SARS-CoV-2 and influenza viruses, JAMA Netw. Open 5 (1) (2022) e2145669, https://doi.org/10.1001/jamanetworkopen.2021.45669.
[106] P. Akarapipad, et al., Smartphone-based sensitive detection of SARS-CoV-2 from saline gargle samples via flow profile analysis on a paper microfluidic chip, Biosens. Bioelectron. 207 (2022) 114192, https://doi.org/10.1016/j.bios.2022.114192.
[107] Y.Q. Xia, et al., Smartphone-based point-of-care microfluidic platform fabricated with a ZnO nanorod template for colorimetric virus detection, ACS Sens. 4 (12) (2019) 3298–3307, https://doi.org/10.1021/acssensors.9b01927.
[108] Y. Minagawa, et al., Mobile imaging platform for digital influenza virus counting, Lab Chip 19 (16) (2019) 2678–2687, https://doi.org/10.1039/c9lc00370c.
[109] E.M. Materon, et al., Colorimetric detection of SARS-CoV-2 using plasmonic biosensors and smartphones, ACS Appl. Mater. Interfaces 14 (49) (2022) 54527–54538, https://doi.org/10.1021/acsami.2c15407.
[110] Y.D. Ma, et al., An integrated self-driven microfluidic device for rapid detection of the influenza A (H1N1) virus by reverse transcription loop-mediated isothermal amplification, Sens. Actuators B Chem. (2019) 296, https://doi.org/10.1016/j.snb.2019.126647.
[111] L. Shi, et al., Ultrasensitive and facile detection of microRNA via a portable pressure meter, ACS Appl. Mater. Interfaces 10 (15) (2018) 12526–12533, https://doi.org/10.1021/acsami.8b02551.